Erbium in crystal silicon: Segregation and trapping during solid phase epitaxy of amorphous silicon

J. S. Custer,[a] A. Polman, and H. M. van Pinxteren
FOM Institute for Atomic and Molecular Physics, Kruislaan 407, 1098 SJ Amsterdam, The Netherlands

(Received 20 August 1993; accepted for publication 16 November 1993)

Solid phase epitaxy of Er-implanted amorphous Si results in segregation and trapping of the Er, incorporating up to 2×10^{20} Er/cm^3 in single-crystal Si. Segregation occurs despite an extremely low Er diffusivity in bulk amorphous Si of $\leqslant10^{-17}$ cm^2/s, and the narrow segregation spike (measured width ≈3 nm) suggests that kinetic trapping is responsible for the nonequilibrium concentrations of Er. The dependence of trapping on temperature, concentration, and impurities indicates instead that thermodynamics controls the segregation. We propose that Er, in analogy to transition metals, diffuses interstitially in amorphous Si, but is strongly bound at trapping centers. The binding enthalpy of these trapping sites causes the amorphous phase to be energetically favorable for Er, so that at low concentrations the Er is nearly completely segregated. Once the concentration of Er in the segregation spike exceeds the amorphous trap center concentration, though, more Er is trapped in the crystal. We also observe similar segregation and trapping behavior for another rare-earth element, Pr.

I. INTRODUCTION

There has been much interest in obtaining light emission from crystal Si (*c*-Si) through the introduction of luminescing rare-earth dopants. Work has focused on erbium because the luminescence occurs near 1.5 μm, a standard optical communication wavelength.[1–8] Making technologically useful devices requires incorporation of at least $\sim10^{18}$/cm^3 of Er in the *c*-Si host.[9] Using near-equilibrium crystal growth processes will limit impurity incorporation to the maximum solid solubility. Unfortunately, the solubilities of rare earths in *c*-Si have not, as a rule, been measured, although by analogy to the transition metals they are likely to be low ($\approx10^{14}$–10^{16}/cm^3).[10] This implies that nonequilibrium processing methods must be used to obtain Er concentrations that are high enough for optoelectronic devices.

Phase transitions usually result in segregation, the redistribution of an impurity at a moving phase boundary. In general, segregation is characterized by the segregation coefficient k, defined as the ratio of impurity concentrations on either side of the moving interface. Near equilibrium, k is determined thermodynamically by the ratio of the impurity solubilities in the two phases, called k_e. If k is less than 1 and the impurity can diffuse ahead of the interface, a segregation spike forms which contains the impurity rejected from the growing phase. Equilibrium segregation is observed in such processes as zone-melt refining.[11] Far from equilibrium, however, kinetic factors can increase the trapping. Kinetic trapping occurs when impurities are unable to diffusively escape incorporation in the growing phase, increasing the trapping so that $k>k_e$.[12,13] An indicator for kinetic trapping is the segregation spike width, approximated by D/v, where D is the impurity diffusivity ahead of the interface and v is the interface velocity. When $D/v\leqslant10$ nm, kinetic trapping is readily observed in Si in extremely nonequilibrium processes like pulsed laser annealing (liquid/solid transition) and ion-beam-induced epitaxial crystallization (amorphous/crystal transition). Both of these processes have been used to incorporate high concentrations of metals in *c*-Si.[14–20]

Recently, we have demonstrated that segregation and trapping during solid phase epitaxy (SPE) of Er-doped amorphous Si (*a*-Si) can incorporate up to 10^{20} Er/cm^3 in *c*-Si.[21] In this paper, we will discuss more detailed measurements of this process, including the diffusivity of Er in bulk *a*-Si, the effects of Er segregation on the SPE rate, the profile of the segregation spike itself, as well as the effects of temperature, concentration, and impurities on the trapping levels of Er. These experiments were performed in order to understand what controls the incorporation of Er in *c*-Si. The measured segregation spike width of ≈3 nm suggests that kinetic trapping is important. However, the changes in the segregation coefficient with Er concentration, temperature, and the presence of coimplanted oxygen indicates instead that k is determined primarily by thermodynamic, not kinetic factors. We also show that another rare earth, Pr, can be incorporated in *c*-Si in a similar manner. Praseodymium exhibits luminescent transitions 1.3 μm in other hosts, so this may also allow the fabrication of Si-based devices at this optical communication wavelength.

II. EXPERIMENTAL

Erbium was incorporated in *a*-Si by implanting Er either directly into *c*-Si (4 and 9×10^{14}/cm^2 250 keV Er) or into *a*-Si previously made by Si implantation (3×10^{15}/cm^2 350 keV Si followed by 8×10^{13}, 8×10^{14}, 1.3, 2.4, or 5.4×10^{15}/cm^2 250 keV Er). The Si(100) substrates used for these samples were Czochralski-grown and either P doped (1.1–1.45 Ω cm) or B doped (5–10 Ω cm). The Er implants in *c*-Si generated amorphous layers ≈160 nm

[a]Present address: Sandia National Labs, M/S 1056, Albuquerque, NM 87185.

 0021-8979/94/75(6)/2809/9/$6.00

thick, while the Si preamorphized layers were 500 nm thick. In addition, thicker (780 nm) *a*-Si layers were made by 5×10^{15}/cm^2 keV Si implants in float-zone grown B-doped (0.2 Ω cm) Si(100), followed by 0.6 or 1.6×10^{15}/cm^2, 1.5 MeV Er implants. Praseodymium-doped *a*-Si layers were made by implanting 3.5 or 7.0×10^{14}/cm^2 250 keV Pr into *c*-Si (Czochralski-grown as above), resulting in $\approx$160-nm-thick *a*-Si layers. All implants were performed with the samples heat sunk to a copper block cooled by liquid nitrogen.

Anneals were performed either in a vacuum furnace (base pressure 10^{-7} Torr) or a rapid thermal annealer. Rapid thermal anneals were done under flowing Ar. The time to reach the anneal temperature was 5 s; all indicated anneal times are after the anneal temperature was reached.

The amorphous layer thicknesses and impurity concentration profiles were measured with Rutherford backscattering spectrometry (RBS) in the channeling geometry using 2 MeV Hc. A backscattering angle of 100° was used to give a depth resolution of better than 10 nm on thin layers, using a surface barrier detector cooled to 0 °C (<16 keV energy resolution). The thick *a*-Si layers were analyzed using a backscattering angle of 165°. For these samples, the Er profiles were measured under random conditions to ensure consistent depth scales, necessary because of the difference in stopping between random and channeled He ions. Medium-energy ion scattering (MEIS) was performed with 100 keV protons. A two-dimensional position sensitive detector on a toroidal electrostatic energy analyzer recorded the energy and scattering angle. The energy resolution was 90 eV ($\Delta E/E = 9\times10^{-4}$), providing a depth resolution of less than a monolayer at the sample surface,[22] although energy straggling degrades the resolution for deeper depths.

III. RESULTS

A. Segregation of erbium

Figure 1 shows the Er portion of RBS spectra of the 4×10^{14} Er/cm^2 sample after rapid thermal anneals (RTAs) for various times at 600 °C.[23] The as-implanted Er profile is approximately Gaussian, peaked at a depth of 70 nm with a FWHM of 60 nm. For annealed samples, the *a*-Si/*c*-Si interface moves towards the surface via SPE. The position of the interface is indicated by the arrows for each time. As the *a*-Si/*c*-Si interface moves through the Er profile, the Er is pushed ahead of the interface, building up a large concentration at the interface (the width of the segregation spike is detector-resolution limited). Eventually, Er starts to be trapped in the crystal. At the end, the segregation spike of Er is deposited at the surface. SPE clearly leads to segregation and trapping of Er.

Figure 2 shows both the Si and Er portions of RBS/channeling spectra after 15 min, 600 °C anneals of samples implanted with different Er fluences. Single-crystal regrowth to the surface is observed only for the two lowest Er doses (4 and 9×10^{14} Er/cm^2). For higher Er doses, the higher channeling yield in the Si surface region [Fig. 2(a)] indicates a breakdown of SPE to nonperfect crystal

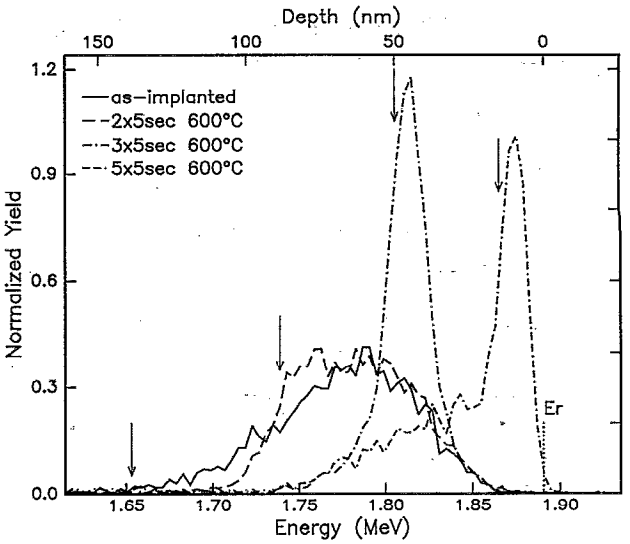

FIG. 1. RBS spectra of the 4×10^{14} Er/cm^2 sample as implanted, and after 2, 3, or 5 RTA anneals of 5 s each at 600 °C. The arrows indicate the position of the *c*-Si/*a*-Si interface as determined from the Si portion of each spectrum. As the interface moves through the Er profile, Er is segregated at the interface with a portion remaining trapped behind in the crystal.

growth. This region has been shown to be heavily twinned.[21] The higher the Er dose, the earlier the breakdown of SPE occurs during regrowth. A comparison of the concentration of Er in the *c*-Si at the time of breakdown [Fig. 2(b)] indicates that trying to trap more than 1.2×10^{20} Er/cm^3 results in twinned crystal. Once twinning occurs, the trapping of Er in the *c*-Si increases rapidly.

Figure 3 shows the Si and Er portions of RBS/channeling spectra following 100 h, 500 °C furnace anneals of samples with various Er fluences. From the Si portion of the spectra [Fig. 3(a)] it can be seen that now the 1.3×10^{15} Er/cm^2 sample regrows to the surface, in contrast to the 600 °C anneal [Fig. 2(a)]. However, 500 °C anneals of higher Er doses (2.4×10^{15} Er/cm^2) again lead to heavily defected crystal regrowth. Figure 3(b) demonstrates that the maximum trapped Er concentration before breakdown, 2×10^{20} Er/cm^3, is roughly twice as high as 500 °C than at 600 °C. Similar experiments for 900 °C RTAs (not shown) yields a maximum trapped concentration of only 6×10^{19} Er/cm^3. Although the solubility limit of Er in *c*-Si has not been measured, by analogy to the transition metals it is likely to be relatively small ($\sim10^{14}$–10^{16} Er/cm^3).[10] This indicates that the trapped concentrations obtainable during SPE ($>1\times10^{20}$ Er/cm^3) are far above equilibrium.

None of the SPE-recrystallized samples exhibit a difference in the Er RBS yield between random and (100) channeled spectra, indicating that Er is not substitutional in the *c*-Si. This lack of a channeling effect also demonstrates that Er does not occupy the tetrahedral interstitial site. Channeling studies on other crystallographic directions are required before any firm conclusion can be made about what site Er occupies. However, these results, ob-

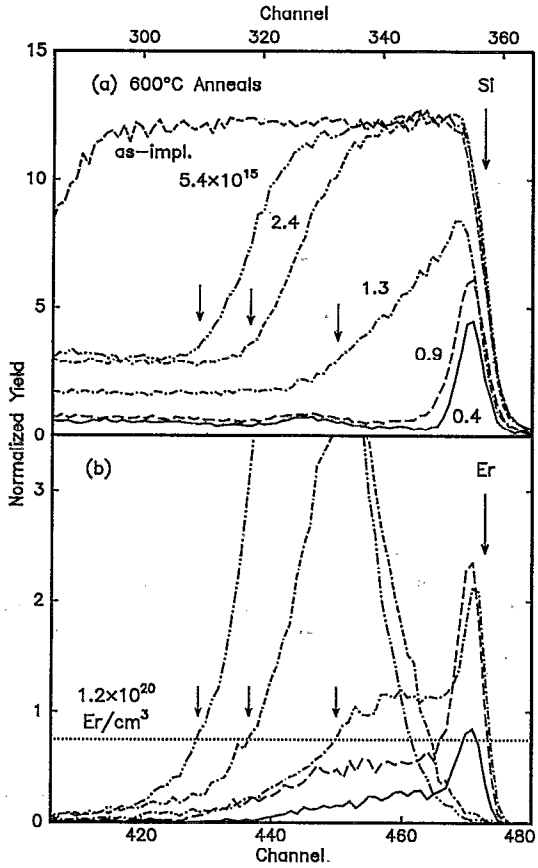

FIG. 2. The (a) Si and (b) Er portions of RBS spectra after annealing Er implanted a-Si for 15 min at 600 °C. The channel scales are plotted such that Si and Er have the same relative depth scale. A comparison of the Er concentration when twin formation occurs (arrows) shows that the maximum Er concentration in single-crystal Si is 1.2×10^{20} Er/cm^3 (dotted line). Trying to trap concentrations higher than this results in twin formation, leading to the increase in dechanneling in the Si portion of the spectra.

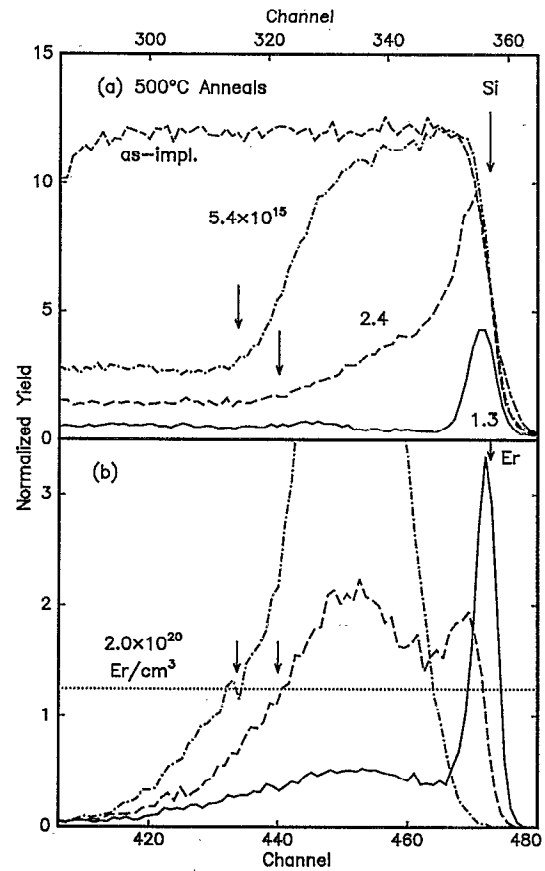

FIG. 3. The (a) Si and (b) Er portions of RBS spectra after annealing Er implanted a-Si at 500 °C for 100 h. The channel scales are plotted such that Si and Er have the same relative depth scale. The arrows and dotted lines in the Er portion show that the maximum concentration of Er trapped in single-crystal Si is 2×10^{20} Er/cm^3, higher than for 600 °C.

tained for Er concentrations that we believe are far above the solid solubility limit, may not be indicative of the lattice site location for low Er concentrations.

Changing the temperature also changes the segregation characteristics. A comparison of the Er profiles of the 1.3×10^{15} Er/cm^2 sample annealed at 500 °C [Fig. 3(b)] and the 9×10^{14} Er/cm^2 sample annealed at 600 °C [Fig. 2(b)] shows that the 500 °C anneal traps more Er during the early stages of regrowth (below channel 440), although the peak trapped concentrations (near channel 450) are almost the same. The trapping of Er also depends on the Er concentration. Figure 4 shows RBS spectra after 15 min, 600 °C anneals of samples with 8×10^{13} or 8×10^{14} Er/cm^2 implanted in a-Si. The profile for the higher dose sample (8×10^{14} Er/cm^2) exhibits segregation similar to that shown in Fig. 2. However, in the lower dose sample, essentially all of the Er has segregated to the surface. The results in Fig. 4 show that k is very different for samples implanted with different Er doses, so k is concentration dependent. This can also be seen in the profiles in Fig. 1. In the initial stages of regrowth all of the Er segregates forward. It is only after the segregation spike has passed the peak of the Er implant profile and accumulated a large concentration of Er in the segregation spike that substantial trapping occurs. For the low dose Er implant in Fig. 4, the Er concentration in the spike apparently never became large enough to cause an increase in k. Thus, for low implantation doses of Er, nearly complete segregation is observed. At intermediate doses, the concentration of Er in the segregation spike becomes large enough so that k increases and trapping of high concentrations of Er in the crystal occurs. At a particular, temperature-dependent trapping level of Er in the crystal (which should imply in turn a specific concentration of Er ahead of the interface in the segregation spike), the single-crystal regrowth breaks up through the formation of twins, and the trapping of Er increases.

B. Effect of erbium on the SPE velocity

To measure the effect of Er on the SPE rate, we performed anneals on the thicker a-Si layers. These had Gaussian Er profiles centered on a range of 440 nm with a FWHM of 270 nm. Anneals were carried out for various times in a vacuum furnace at either 525 or 550 °C, with each anneal consisting of pieces of the Er-implanted samples together with pure a-Si. The remaining a-Si thick-

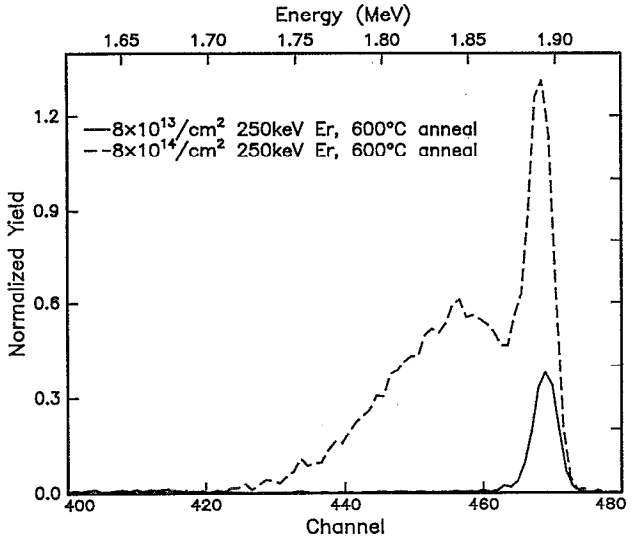

FIG. 4. RBS spectra after annealing for 15 min at 600 °C of *a*-Si layers implanted with 8×10^{13} or $8\times10^{14}/\text{cm}^2$ 250 keV Er. During SPE, a majority of the Er in the higher dose sample is trapped in the *c*-Si. In contrast, almost all of the Er has segregated to the surface in the low dose sample.

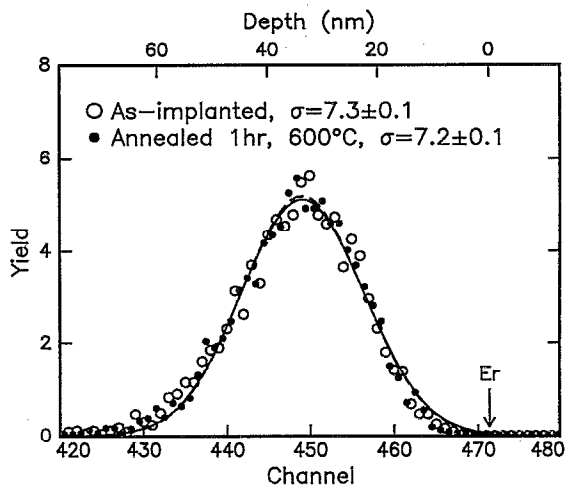

FIG. 6. RBS spectra before and after a 1 h 600 °C anneal of $3\times10^{15}/\text{cm}^2$ 75 keV Er implanted in preamorphized SIMOX. The peak Er concentration is 2 at. %. In this glancing angle geometry, one channel corresponds to 1.5 nm of *a*-Si. The drawn lines are Gaussian fits with the standard deviations σ indicated in the figure. There is no statistically significant difference between the two Er profiles, demonstrating that Er diffuses very slowly.

nesses after annealing were measured with RBS in the channeling configuration. The Er profiles were measured under random conditions to ensure consistent depth scales in the *c*-Si.

Figure 5 shows the amount of *a*-Si regrowth versus anneal time at 525 °C for the pure and Er-implanted *a*-Si samples. The regrowth of a pure *a*-Si is linear in time with a velocity of 0.29 ± 0.02 Å/s, in good agreement with previous measurements.[24] The two Er-implanted samples also regrow at this same velocity as long as the *c*-Si/*a*-Si interface is moving through *a*-Si without any Er in it. Once the *c*-Si/*a*-Si interface reaches the Er profile and Er segregation begins, the regrowth velocity increases to 0.48 ± 0.04 Å/s, 65% higher than for the pure *a*-Si sample. The two Er samples reach the same velocity, although the lower fluence sample achieves it somewhat later than the higher Er fluence sample. The same velocity enhancement factor of 65% is also observed for 550 °C anneals (not shown).

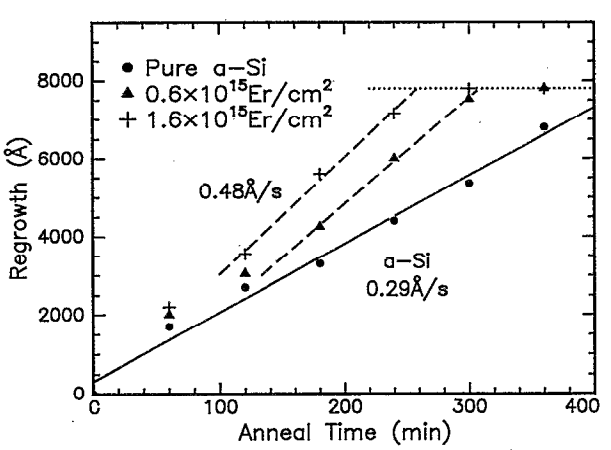

FIG. 5. Regrown thickness vs anneal time at 525 °C for pure *a*-Si and *a*-Si implanted with 0.6 or 1.6×10^{15} 1.5 MeV Er. The dotted line indicates the original *a*-Si layer thickness. The pure *a*-Si regrowth is linear with a velocity of 0.29 ± 0.02 Å/s. The velocity in the Er doped samples increases to 0.48 ± 0.04 Å/s during the segregation of the Er.

C. Erbium diffusivity in amorphous silicon

Because no diffusion of the Er trapped in *c*-Si is observed, the *c*-Si diffusion coefficient of Er is small enough to be neglected in the segregation analysis. The diffusion of the impurity ahead of the advancing interface is, however, crucial to modeling the segregation. To try to measure the Er diffusivity, samples with 120 nm Si on 480 SiO_2 made by the SIMOX process were amorphized by a $1\times10^{15}/\text{cm}^2$ 100 keV Si implant at liquid nitrogen temperature. SIMOX was used to avoid solid phase recrystallization of the amorphized films during the 600 °C anneals used for the diffusion studies. A $3\times10^{15}/\text{cm}^2$ 75 keV Er implant (peak concentration of 2 at. % Er), also at liquid nitrogen temperature, was used to make a shallow Gaussian Er profile for measuring diffusion.

Figure 6 shows the Er portion of RBS spectra taken at glancing angle (97° backscattering angle) before and after a 1 h 600 °C anneal. Transmission electron microscopy and diffraction (not shown) show that the sample is still amorphous after the anneal. Gaussian fits to the two spectra result in rms deviations of $\sigma=7.3\pm0.1$ channels before annealing and $\sigma=7.2\pm0.1$ channels after annealing. Therefore, the Er profiles before and after annealing are statistically the same. Since one channel is equivalent to 1.5 nm, this indicates that the diffusion coefficient of Er in bulk *a*-Si at 600°C is less than 1×10^{-17} cm²/s.

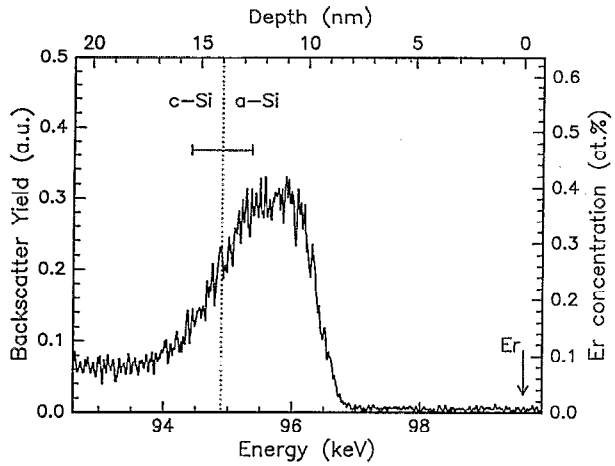

FIG. 7. The Er portion of a MEIS spectrum from a 4×10^{14} Er/cm^2 sample regrown to 14 nm from the surface (5×5 s at 600 °C, see Fig. 1). The Er surface energy is indicated by the arrow. The position of the c-Si/a-Si interface (dotted line) is within the range shown by the bar. The segregation coefficient derived from the Er concentrations in the a-Si and c-Si is $k\approx0.2$.

D. Measuring the segregation spike width

Combining the interface velocity during recrystallization (1 nm/s, as estimated from Fig. 1) with the maximum diffusivity estimated above yields a segregation spike width of $D/v\approx10^{-3}$ nm. This is an unphysical spike width because it is much less than an interatomic spacing in Si. Using MEIS it is possible to directly measure the segregation spike profile, provided that it is very near the surface. The short-time 600 °C RTAs of the 4×10^{14} Er/cm^2 sample resulted in a sample where the a-Si/c-Si interface was only ≈14 nm from the surface (5×5 s anneal in Fig. 1). For the MEIS measurements, 100 keV H ions were incident several degrees off a [111] direction, and collected over a 20° angular range. In this geometry, there is no channeling of the incident beam, but blocking of the backscattered protons in the crystal substrate can be observed (not shown).

Figure 7 shows the Er portion of the MEIS spectrum for this sample at a scattering angle of 103.3°. The Er surface energy is indicated by the arrow. Since the blocking dips in the c-Si are relatively shallow, and because the Si signal lies atop a (nonconstant) Er background, it is difficult to determine the exact position of the a-Si/c-Si interface from the Si portion of the MEIS spectrum. The dotted line indicates the position of the interface determined from 2 MeV He channeling data, with the error bar resulting from uncertainties in the stopping cross sections for both 100 keV H and 2 MeV He. The Er concentration trapped in the crystal is 4.5×10^{19} Er/cm^3, while the concentration in the a-Si directly ahead of the interface is 2×10^{20} Er/cm^3, some $5\times$ higher ($k\approx0.2$). The width of the segregation spike is ≈3 nm, significantly larger than estimated above from the bulk a-Si diffusivity and interface velocity. In addition to being wider than expected, the shape of the segregation spike is noteworthy, with a sharp leading edge in the a-Si and a broader trailing edge at the a-Si/c-Si interface. This is the opposite of the classic segregation spike shape of a leading edge broadened by diffusion into the a-Si and a sharp step at the c-Si/a-Si interface.

Three different factors can influence the measured shape of the profile: the detector resolution, energy straggling of the H beam, and thickness variations in the a-Si overlayer over the diameter of the H beam (~1 mm). The detector resolution is almost entirely negligible relative to the widths of the leading or trailing edges.[22] Any variations in the thickness of the a-Si layer would smear out the entire profile, which is inconsistent with the sharp leading edge. The sharpness of the rising edge places an upper limit on the energy straggling. Fits of trial profiles (not shown) assuming either no energy straggle, or that the width of the rising edge is determined entirely by straggling, result in segregation spike widths (FWHM) of 3.4 and 2.8 nm, respectively.

In all fits, the front edge of the segregation spike is sharper than the trailing edge, and this does not result from the factors discussed above. The rms roughness of an (impurity free) a-Si/c-Si interface has been measured, using x-ray diffraction, to be <1 nm.[25] However, this could only account for some of the width of the trailing edge. Further, it would require that Er diffuses rapidly parallel to the interface to keep the front edge sharp. This type of diffusion behavior is unlikely to occur in the isotropic a-Si. Another possibility is that there is a transition region in the a-Si between the a-Si/c-Si interface and the bulk a-Si film. Then, the width of the trailing edge of the Er profile would occur through, e.g., a decrease in trap density through the transition region. Although a transition region is required to accommodate bonding constraints, it is generally thought to be at most a few atomic layers thick,[26–28] much thinner than is required here. In any case, the actual segregation spike profile is asymmetric, with the leading edge being sharper than the trailing edge.

E. Effects of oxygen on erbium segregation

It has been shown that oxygen affects the segregation and trapping of Er during SPE.[29] In order to investigate what happens when an Er segregation spike encounters an O-rich region, thick a-Si samples implanted with 1.5 MeV Er (as used for the SPE velocity measurements) were coimplanted with 5×10^{15}/cm^2 160 keV oxygen. This energy was chosen to place the O profile slightly close to the surface than the Er profile, as sketched schematically in Fig. 8(b). The O peak concentration was 1.5×10^{20}/cm^2. Samples implanted only with Er, and oxygen coimplanted samples were annealed at 550 °C. RBS-channeling measurements (not shown) of partially regrown samples show that the presence of the O retards SPE, as expected for O alone.[30] Figure 8(a) shows RBS spectra of the as-implanted Er profile, and the profile after SPE at 550 °C of the sample implanted only with Er. The SPE results in significant segregation, with the ER segregation spike reaching all the way to the surface (note that the depth scales are very different than in Figs. 1–4). Figure 8(b) shows RBS spectra for the Er+O sample after 1 and 11 h anneals at 550 °C. Before the interface reaches the im-

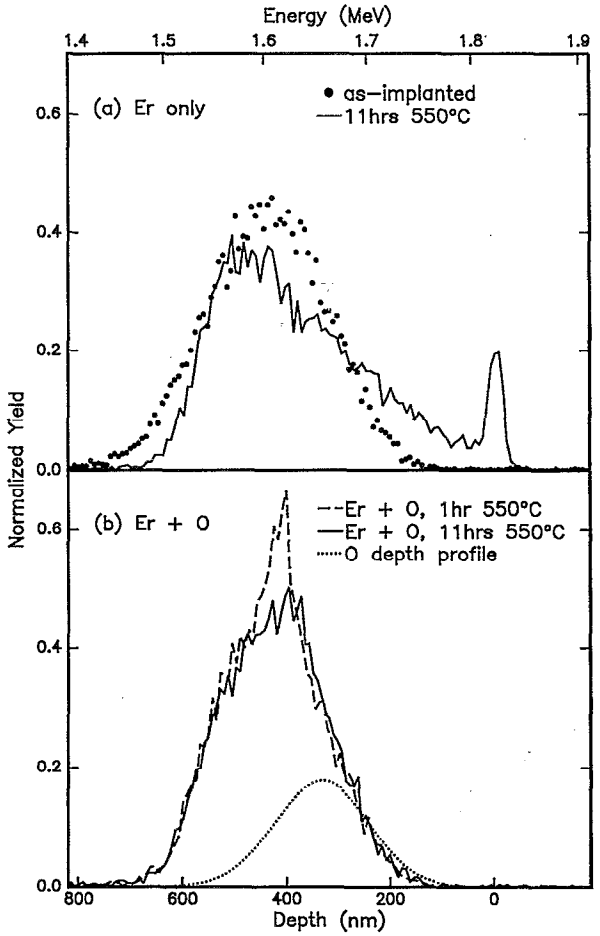

FIG. 8. (a) RBS spectra of 780-nm-thick *a*-Si as implanted with 1.6×10^{15}/cm^2 1.5 MeV Er, and after SPE at 550 °C. Considerable segregation of the Er is observed. (b) RBS spectra of 780-nm-thick *a*-Si implanted with 1.6×10^{15}/cm^2 1.5 MeV Er and 5×10^{15}/cm^2 160 keV O after annealing for 1 h and 11 h at 550 °C. A small segregation spike is observed for the 1 h anneal. After the 11 h anneal, no Er has been segregated to the surface as is observed in (a) for the sample without any O. The shape and position of the implanted O profile is schematically indicated by the dotted curve.

planted O, the segregation and trapping of Er are similar to that in the sample without additional O. However, as the interface grows through the O profile, the trapping increases dramatically, and no Er reaches the sample surface. This shows that the segregation coefficient (the trapping) must be higher in the oxygen coimplanted sample. However, segregation occurs initially, as demonstrated by the presence of a segregation spike in the 1 h annealed sample.

F. Segregation and trapping of praseodymium

To determine if the segregation and trapping of Er is a general property of the rare-earth elements, we attempted to incorporate Pr in *c*-Si. Figure 9 shows the Pr region of RBS spectra before and after annealing (1 h at 550 °C) of Pr-implanted *a*-Si. For a low dose (3.5×10^{14}/cm^2 250 keV Pr) implant, almost complete segregation to the surface is observed. The higher dose (7×10^{14} Pr/cm^2 250 keV Pr) sample leads to much more trapping of Pr in the *c*-Si. The

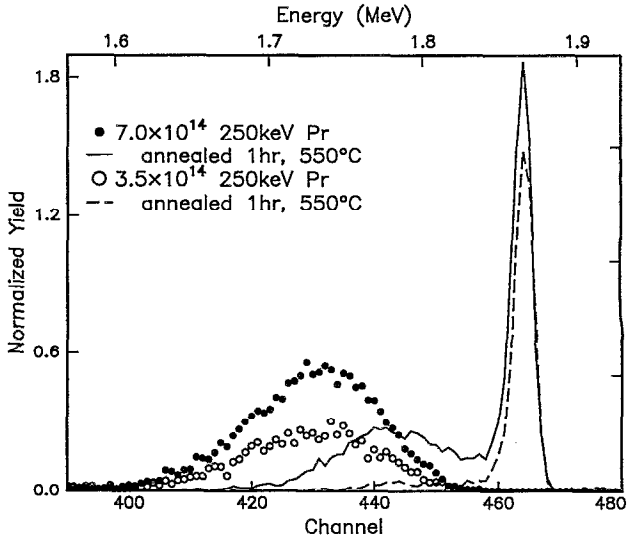

FIG. 9. The Pr region of RBS spectra before and after 1 h 550 °C anneals of *a*-Si implanted with 3.5 and 7×10^{14} 250 keV Pr. The anneal results in complete recrystallization of the *a*-Si layer by SPE, and segregation and trapping of the Pr. The maximum trapped Pr concentrations are 7.5×10^{18} and 5.5×10^{19} Pr/cm^3 for the two samples.

peak trapped concentrations are 7.5×10^{18} and 5.5×10^{19} Pr/cm^3 for the Pr doses of 3.5 and 7.0×10^{14} Pr/cm^2, respectively. Both samples exhibit single-crystal growth to the surface, as is also observed for Er at similar concentrations and anneal temperatures. The large increase in trapping with Pr dose is also similar to what is observed for Er (Fig. 4).

IV. DISCUSSION

Previous examples of impurity redistribution in Si during SPE can be split into three different cases. At one extreme, the impurity has a very low diffusivity and does not redistribute, resulting in complete trapping, even at concentrations several orders of magnitude above the solid solubility.[31,32] This generally occurs for dopants (e.g., B, P, As, and Sb) which are placed on substitutional lattice sites during growth. A second extreme is observed for fast diffusing metals (i.e., Cu, Ag, and Au) where the impurity is completely rejected from the growing crystal.[33,34] The increasing concentration of the metal in the *a*-Si eventually disrupts epitaxy. In the case of Au, this occurs by nucleation of twins at the growing interface, with Au being trapped in the twinned crystal. For Cu and Ag, epitaxy is instead halted by random nucleation of crystal in the *a*-Si layer. Finally, In is a special segregation case. At low In concentrations, the In is completely trapped on substitutional lattice sites.[35] Above a critical concentration, a narrow segregation spike forms which sweeps the excess In towards the surface.[36–38] Finally, at even higher concentrations a rapid, melt-mediated crystallization of the *a*-Si layer is observed. The trapping of In is affected by codoping with other elements, possibly by changing the effective solubility limit of In in *c*-Si.[36]

The segregation and trapping of Er differs in general

from these three cases. The diffusivity of Er in *a*-Si is so small ($<10^{-17}$ cm^2/s) that complete trapping is expected, but segregation is observed instead. The segregation coefficient is sensitive to parameters such as temperature, concentration, and coimplanted impurities. Finally, the segregation spike profile is unlike what is expected for classic segregation. Determining the physical reasons for these experimental observations is difficult because there is very little known about Er in either *a*-Si or *c*-Si, such as the diffusion mechanisms, diffusivities, impurity solubilities, and the thermodynamics of Er in *c*-Si versus *a*-Si, which determine if the trapping is thermodynamic or kinetic. Using what is known about the behavior of transition metals in *a*-Si, and the physical properties of *a*-Si itself, we present below a possible scenario which explains the segregation and trapping of Er in *c*-Si.

A. Diffusivity of erbium

The attempt to measure the diffusivity of Er in bulk *a*-Si (Fig. 6) indicated that the diffusivity is $<1\times10^{-17}$ cm^2/s at 600 °C. This is far too small to allow significant segregation, much less to account for the measured segregation spike width, implying that the Er diffusivity near the *a*-Si/*c*-Si interface must be enhanced with respect to the bulk value. There has been much recent work on the diffusion mechanism of transition metals in *a*-Si,[39–42] which may apply as well to the metallic rare earths. The transition metals are believed to diffuse interstitially, but are "retarded by temporary trapping at defects intrinsic to the amorphous structure."[42] The diffusion rate depends strongly on the concentration and strength of the traps.

If Er diffuses in a manner analogous to the transition metals, then we can qualitatively explain a diffusivity enhancement near the *a*-Si/*c*-Si interface by enhanced detrapping during SPE of Er occupying traps in the *a*-Si. This may occur in two ways. First, detrapping will occur as the *c*-Si/*a*-Si interface reaches an occupied trap and consumes it, rejecting the Er as an interstitial. Second, some detrapping in the vicinity of the interface may also occur through the bond rearrangements at or near the *a*-Si/*c*-Si interface that cause SPE.[24,43] Some bond rearrangements may take place just ahead of the interface to maintain a constant bond density at the interface.[28] In any case, Er near the interface is able to diffuse because it is ejected from the traps by the growth process itself, while Er in the bulk *a*-Si remains trapped. The ejected Er will diffuse until encountering an empty trap in the *a*-Si, or being incorporated in the growing *c*-Si.

An estimate of the diffusivity at 600 °C of Er near the interface can be obtained from the MEIS spectrum in Fig. 7. Using the approximation that, in a normal segregation process, the segregation spike width is D/v, and using the measured width of some 3 nm and a regrowth velocity of 1 nm/s, the diffusivity required to keep the spike moving is on the order of 3×10^{-14} cm^2/s. This is at least three orders of magnitude higher than the upper bound on the bulk diffusivity of Er in *a*-Si obtained from Fig. 6. Although it is difficult to draw firm conclusions without good data on the Er diffusivity in *c*-Si, it is apparent that Er is strongly bound to the traps in the bulk *a*-Si. This strong interaction with the traps can also have large effects on the segregation process, not just the diffusivity.

B. Thermodynamic versus kinetic trapping

For low Er doses, nearly complete segregation of Er to the surface is observed (Fig. 4). It is only for higher doses that k increases and substantial trapping is observed. To determine why k changes we must determine if k is controlled by thermodynamic ($k\approx k_e$) or kinetic ($k>k_e$) factors. The large trapped concentrations of Er, probably well above the solubility limit, coupled with the narrow segregation spike, are suggestive of kinetic trapping. However, this view ignores the amorphous side of the interface, where the solubility of Er is not known either. We suggest that the structural defects in the *a*-Si that limit diffusion will also affect the free energy of impurities. It will be argued below that k is controlled by thermodynamics and that kinetic trapping does not occur. This is also concluded from the changes in k observed in the O coimplanted samples.

The equilibrium segregation coefficient k_e is commonly defined as the ratio of impurity solubilities on either side of the interface. The tie-line construction used to determine phase equilibria (and hence solubility limits) is equivalent to requiring that the chemical potentials of the impurity and the host are constant across the interface. This implicitly assumes that the interface is at or near equilibrium. In the case here, *a*-Si is metastable with respect to *c*-Si at all temperatures below the melting point. Thus, *a*-Si is *never* in equilibrium with *c*-Si.[44] This makes it difficult to define k_e in the standard sense. We instead take "equilibrium" segregation to mean that the impurity redistributes itself so as to keep its own chemical potential constant across the interface. Further, because the segregation process is dynamic and the bulk diffusivity is small, we can only consider local equilibrium near the interface and within the segregation spike itself.

The chemical potential has both entropic and enthalpic contributions, although the entropy of mixing should be essentially the same in *c*-Si and *a*-Si. Because of the similarity in short-range order in *c*-Si and *a*-Si, the enthalpy to place an Er atom on a given position, e.g., interstitially, should also be similar in the two phases. The major difference is the presence in the *a*-Si of the trap sites (0.1–1 at. %) which are important in determining the diffusivity.[40–42] Because of the substantial trapping enthalpy ($\sim$1 eV),[42] Er will preferentially occupy these sites. It is these traps that increase the solubility of Er in *a*-Si relative to *c*-Si.

As long as the Er concentration in the *a*-Si is less than the trap density, the chemical potential of Er in *a*-Si will be less than in *c*-Si, resulting in $k_e\approx0$. (Note that some trapping of Er in the *c*-Si should always occur, if only for entropic reasons.) Any Er atom rejected from the *a*-Si/*c*-Si interface will readily find an unoccupied trap. Once the traps near the interface are filled (within a diffusion length in the Er-saturated *a*-Si), however, the energy difference

between placing Er in (trap saturated) a-Si and c-Si becomes very small. The Er will then diffuse until it finds an unoccupied trap in the a-Si (by diffusing through the trap-saturated a-Si), or it gets left behind in the c-Si as the interface moves away. (It should be noted that the Er in the segregation spike is only in local equilibrium—in true equilibrium the Er would redistribute throughout the a-Si layer.) The result is that k_e should increase with increasing Er concentration, as is observed (see Fig. 4). Thus, kinetic trapping does not have to be invoked to explain the concentration dependence of k.

There is another reason to suspect that the observed segregation is determined by thermodynamic considerations more than kinetics. In the usual kinetic trapping regime (pulsed laser melting) k is determined almost entirely by the interface velocity (k increases with increasing velocity), and is almost independent of k_e.[12,13] However, the samples coimplanted with O show an increased trapping rate even though the SPE rate was lower than in the samples without O. This is contrary to what is expected for kinetic trapping. In this case, the presence of O may make incorporation of Er in the crystal easier, possibly through formation of Er-O complexes which would lower the enthalphy required to introduce Er into c-Si. Alternatively, O could either preferentially occupy or decrease the density of traps in the a-Si. Such an elimination of the traps which Er prefers energetically would increase k by altering the balance of free energies of Er in c-Si and a-Si. Either way, the presence of O affects the equilibrium segregation coefficient. More measurements are underway to distinguish between these alternatives.

C. Segregation spike profile

In classical segregation, the peak of the segregation spike is expected to be at the c-Si/a-Si interface where the Er is rejected from the c-Si. Because the spike width measured here is substantially larger than would be expected from the bulk diffusivity and the regrowth velocity, an enhanced diffusivity of Er near the interface was proposed above. The proposed mechanisms for diffusivity enhancement and thermodynamically controlled segregation can also lead to a segregation spike profile with a flattopped shape. The concentration of Er ahead of the interface will be determined by the trap density plus the excess Er that is attempting to diffuse away from the interface to avoid incorporation in the c-Si. This explains the wide, nearly flattopped nature of the measured segregation spike. Assuming that the Er in c-Si and the excess Er in a-Si have roughly the same concentration (i.e., similar enthalpies), this indicates that the trap density is close to 0.3 at. %, in good agreement with estimates of the trap density as measured by metal diffusion,[42] as well as calorimetry, photocarrier lifetime, and conductivity studies.[45–48] The sharp falloff in concentration at the front of the segregation spike is the result of Er occupying the first available empty trap in the a-Si. The much wider rear edge of the Er segregation spike may be the result of the excess Er diffusing around the c-Si/a-Si interface as it attempts to find an energetically favorable site.

D. SPE velocity effects and breakdown

The segregation of Er leads to a 65% enhancement in the SPE velocity. The reasons for the velocity change are most likely similar to those for the fast diffusing metals (Cu, Ag, and Au), which have been discussed in detail elsewhere.[33,34] These metals are thought to influence SPE through metal–Si interactions altering bond strengths at or near the interface.[49] Since Er interacts strongly with Si, as evidenced by silicide formation at low temperatures (<300 °C),[50] an enhancement in the SPE rate is expected within this model. The velocity enhancement is nearly constant once segregation starts, and is the same for samples with different Er concentrations, which is in agreement with the idea that the concentration of Er directly at the interface quickly saturates at the a-Si trap density. It should be mentioned that since Er enhances the SPE rate there would appear to be no effects of solute drag on the segregation process.

The other effect of Er on SPE is the breakdown of epitaxy via twin formation for high Er concentrations and/or high anneal temperatures. One possible mechanism is disruption of the growth front by Er precipitation or silicidation in the segregation spike immediately ahead of the interface, generating the twins. However, no second phase precipitates can be identified even in high resolution TEM images of the twinned region.[21] Further, no precipitates or silicides can be observed after the 1 h 600 °C anneal of the SIMOX diffusion sample (maximum Er concentration of 2 at. %), which would seem to discount this breakdown mechanism. The second possible mechanism is related to the segregation itself. As the Er concentration in the a-Si and c-Si increases well above the solubility limits, at some point it should become energetically favorable to nucleate twins to use the twin boundaries as Er trapping sites. Once twinning occurs, the segregation coefficient rises sharply, as shown in Figs. 2 and 3, presumably by incorporating Er on the twins. A similar rapid increase in trapping with twin formation has also been observed for Au segregation during SPE or ion-beam-induced epitaxy.[18,33] Still, we are unable to separate cause from effect in this case.

E. Generalization to other rare earths

Initially it would have been surprising to expect *a priori* that other rare earths would be incorporated in c-Si via SPE in a manner similar to Er. This is particularly true since almost nothing is known about the solubilities or diffusivities of rare earths in c-Si or a-Si. For example, changes in the diffusivity in bulk a-Si could completely change the segregation behavior. However, the scenario for Er segregation discussed above is nearly independent of the properties of Er in bulk a-Si. As long as the element diffuses interstitially, and preferentially occupies trapping sites in the a-Si, the scenario may be valid. The only question will be how large the segregation coefficient is, which will mainly depend on how energetically attractive the a-Si traps are for the impurity. Although we cannot be sure at

this stage how similar the segregation of Pr is to Er, the fact that significant trapping of Pr is observed suggests that it may be possible to use SPE to incorporate other rare earths in *c*-Si as well.

V. CONCLUSIONS

In conclusion, SPE can be used to incorporate $\geqslant 1\times 10^{20}$ Er/cm^3 in *c*-Si through segregation and trapping of Er at the moving *a*-Si/*c*-Si interface. Segregation occurs in spite of a very small diffusivity of Er in bulk *a*-Si. The segregation coefficient varies with Er concentration, as well as the presence of coimplanted oxygen. The presence of an Er segregation spike increases the SPE rate by 65%. The scenario suggested for this segregation behavior is that Er prefers to occupy trap sites in a *a*-Si. Segregation occurs through trap annihilation at the interface and injection of Er as a fast diffusing interstitial into the *a*-Si. As long as there is a low concentration of Er in the segregation spike, the diffusing interstitial can find a new trap, and nearly complete segregation is observed. As the Er concentration increases above the trap concentration in the *a*-Si, k increases and the Er concentration trapped in the *c*-Si increases. Segregation and trapping of Pr during SPE is also observed, and the process may be applicable for rare earths in general. However, parameters such as the maximum concentration that can be incorporated may vary from element to element.

ACKNOWLEDGMENTS

We would like to acknowledge E. Snoeks and G. N. van den Hoven for their contributions to this work. This work is part of the research program of the Foundation for Fundamental Research on Matter (FOM) and was made possible by financial support from the Dutch Organization for the Advancement of Research (NWO), the Foundation for Technical Research (STW), and the IC Technology Program (IOP Electro-Optics) of the Ministry of Economic Affairs.

[1] H. Ennen, J. Schneider, G. Pomrenke, and A. Axmann, Appl. Phys. Lett. **43**, 943 (1983).
[2] H. Ennen, G. Pomrenke, A. Axmann, K. Eisele, W. Haydl, and J. Schneider, Appl. Phys. Lett. **46**, 381 (1985).
[3] D. Moutonnet, H. L'Haridon, P. N. Favennec, M. Salvi, M. Gauneau, F. Arnaud D'Avitaya, and J. Chroboczek, Mater. Sci. Eng. B **4**, 75 (1989).
[4] Y. S. Tang and Zhang Jingping, J. Cryst. Growth **102**, 681 (1990).
[5] W. P. Gillin, Zhang Jingping, and B. J. Sealy, Solid State Commun. **77**, 907 (1991).
[6] D. J. Eaglesham, J. Michel, E. A. Fitzgerald, D. C. Jacobson, J. M. Poate, J. L. Benton, A. Polman, Y.-H. Xie, and L. C. Kimerling, Appl. Phys. Lett. **58**, 2797 (1991).
[7] J. L. Benton, J. Michel, L. C. Kimerling, D. C. Jacobson, Y.-H. Xie, D. J. Eaglesham, E. A. Fitzgerald, and J. M. Poate, J. Appl. Phys. **70**, 2667 (1991).
[8] J. Michel, J. L. Benton, R. F. Ferrante, D. C. Jacobson, D. J. Eaglesham, E. A. Fitzgerald, Y.-H. Xie, J. M. Poate, and L. C. Kimerling, J. Appl. Phys. **70**, 2672 (1991).
[9] Y.-H. Xie, E. A. Fitzgerald, and Y. J. Mii, J. Appl. Phys. **70**, 3223 (1991).
[10] F. A. Trumbore, Bell Syst. Tech. J. **39**, 205 (1960).
[11] W. G. Pfann, J. Metals **4**, Trans. AIME **194**, 747 (1952).
[12] M. J. Aziz, J. Appl. Phys. **53**, 1158 (1982).
[13] *Laser Annealing of Semiconductors*, edited by J. M. Poate and J. W. Mayer (Academic, New York, 1982).
[14] A. G. Cullis, H. C. Webber, J. M. Poate, and A. L. Simons, Appl. Phys. Lett. **36**, 320 (1980).
[15] S. U. Campisano and P. Baeri, Appl. Phys. Lett. **42**, 1023 (1983).
[16] M. J. Aziz, J. Y. Tsao, Michael O. Thompson, P. S. Peercy, and C. W. White, Phys. Rev. Lett. **56**, 2489 (1986).
[17] J. M. Poate, J. Linnros, F. Priolo, D. C. Jacobson, J. L. Batstone, and Michael O. Thompson, Phys. Rev. Lett. **60**, 1322 (1988).
[18] F. Priolo, J. L. Batstone, J. M. Poate, J. Linnros, D. C. Jacobson, and Michael O. Thompson, Appl. Phys. Lett. **52**, 1043 (1988).
[19] J. S. Custer, Michael O. Thompson, D. C. Jacobson, and J. M. Poate, Phys. Rev. B **44**, 8774 (1991).
[20] J. S. Custer, A. Polman, E. Snoeks, and G. N. van den Hoven, Mater. Res. Soc. Symp. Proc. **301**, 101 (1993).
[21] A. Polman, J. S. Custer, E. Snoeks, and G. N. van den Hoven, Appl. Phys. Lett. **62**, 507 (1993).
[22] P. M. Zagwijn, Ph. D. thesis, University of Amsterdam, 1993 (unpublished).
[23] In our original paper (Ref. 21) the figure caption of Fig. 1 incorrectly identified these spectra as being from the 9×10^{14} Er/cm^2 implant.
[24] G. L. Olson and J. A. Roth, Mater. Sci. Rep. **3**, 1 (1988).
[25] M. Lohmeier, S. de Vries, J. S. Custer, E. Vlieg, M. S. Finney, F. Priolo, and A. Battaglia (unpublished).
[26] F. Spaepen, Acta Metall. **26**, 1167 (1978).
[27] T. Saito and I. Ohdomari, Philos. Mag. B **43**, 673 (1981).
[28] J. S. Custer, in *Crucial Issues in Semiconductor Materials and Processing Technologies*, edited by S. Coffa (Kluwer Academic, The Netherlands, 1992), p. 477.
[29] S. Coffa, F. Priolo, G. Franzó, V. Bellani, A. Carnera, and C. Spinella, Mater. Res. Soc. Symp. Proc. **301**, 125 (1993).
[30] E. F. Kennedy, L. Csepregi, J. W. Mayer, and T. W. Sigmon, J. Appl. Phys. **48**, 4241 (1977).
[31] S. U. Campisano, E. Rimini, P. Baeri, and G. Foti, Appl. Phys. Lett. **37**, 170 (1980).
[32] J. Narayan, O. W. Holland, and B. R. Appleton, J. Vac. Sci. Technol. B **1**, 871 (1983).
[33] D. C. Jacobson, J. M. Poate, and G. L. Olson, Appl. Phys. Lett. **40**, 118 (1986).
[34] J. S. Custer, Michael O. Thompson, D. J. Eaglesham, D. C. Jacobson, and J. M. Poate, J. Mater. Res. **8**, 820 (1993).
[35] J. S. Williams and R. G. Elliman, Appl. Phys. Lett. **40**, 266 (1982).
[36] R. G. Elliman and Z. W. Fang, J. Appl. Phys. **73**, 3313 (1993).
[37] J. S. Williams and R. G. Elliman, Nucl. Instrum. Methods **182/183**, 389 (1981).
[38] E. Nygren, A. P. Pogany, K. T. Short, J. S. Williams, R. G. Elliman, and J. M. Poate, Appl. Phys. Lett. **52**, 439 (1988).
[39] J. M. Poate, D. C. Jacobson, J. S. Williams, R. G. Elliman, and D. O. Boerma, Nucl. Instrum. Methods B **19/20**, 480 (1987).
[40] A. Polman, D. C. Jacobson, S. Coffa, J. M. Poate, S. Roorda, and W. C. Sinke, Appl. Phys. Lett. **57**, 1230 (1990).
[41] S. Coffa, J. M. Poate, D. C. Jacobson, and A. Polman, Appl. Phys. Lett. **58**, 2916 (1993).
[42] S. Coffa, J. M. Poate, D. C. Jacobson, W. Frank, and W. Gustin, Phys. Rev. B **45**, 8355 (1992).
[43] G. Q. Lu, E. Nygren, and M. J. Aziz, J. Appl. Phys. **70**, 5323 (1991).
[44] We ignore the possibility of an impurity stabilizing *a*-Si with respect to *c*-Si, as there are no examples of this that we are aware of, particularly at low impurity concentrations.
[45] S. Roorda, W. C. Sinke, J. M. Poate, D. C. Jacobson, S. Dierker, B. S. Dennis, D. J. Eaglesham, F. Spaepen, and P. Fuoss, Phys. Rev. B **44**, 3702 (1991).
[46] P. A. Stolk, L. Calcagnile, S. Roorda, W. C. Sinke, A. J. M. Bernsten, and W. F. van der Weg, Appl. Phys. Lett. **60**, 1688 (1992).
[47] Jung H. Shin, J. S. Im, and H. A. Atwater, Mater. Res. Soc. Symp. Proc. **235**, 21 (1992).
[48] S. Coffa, F. Priolo, and A. Battaglia, Phys. Rev. Lett. **70**, 3756 (1993).
[49] D. C. Jacobson, R. G. Elliman, J. M. Gibson, G. L. Olson, J. M. Poate, and J. S. Williams, Mater. Res. Soc. Symp. Proc. **74**, 327 (1987).
[50] J. A. Knapp, S. T. Picraux, C. S. Wu, and S. S. Lau, J. Appl. Phys. **58**, 3747 (1985).